# Seismic retrofitting of existing RC buildings:

# a rational selection procedure based on Genetic Algorithms

**Roberto Falcone**

University of Salerno, Dept. of Civil Engineering, via Giovanni Paolo II n.132, 84084 Fisciano (SA), Italy.

e-mail: rfalcone@unisa.it

**Francesco Carrabs**

University of Salerno, Dept. of Mathematics, via Giovanni Paolo II n.132, 84084 Fisciano (SA), Italy.

e-mail: fcarrabs@unisa.it

**Raffaele Cerulli**

University of Salerno, Dept. of Mathematics, via Giovanni Paolo II n.132, 84084 Fisciano (SA), Italy.

e-mail: raffaele@unisa.it

**Carmine Lima**

University of Salerno, Dept. of Civil Engineering, via Giovanni Paolo II n.132, 84084 Fisciano (SA), Italy.

e-mail: clima@unisa.it

**Enzo Martinelli***

University of Salerno, Dept. of Civil Engineering, via Giovanni Paolo II n.132, 84084 Fisciano (SA), Italy.

e-mail: e.martinelli@unisa.it

*Corresponding author

# Abstract

Reinforced Concrete (R.C.) structures built in the past decades in earthquake-prone regions do not generally meet the seismic safety standards requested by the current codes. Therefore, they generally need to be retrofitted with the aim to reduce their seismic vulnerability within acceptably low levels. Although several technical solutions are nowadays available on the market, the design of retrofitting interventions is mainly based on the so-called “engineering judgment” and, hence, it is highly subjective in nature, yet being bound to respecting strict code provisions. This paper proposes a rational procedure, based on the application of Genetic Algorithms (GAs), intended at selecting the “cheapest” retrofitting solution among the technically feasible ones. The paper shows how the main GA operators (namely, selection, crossover, and mutation) operates on the candidate retrofitting solutions, which, in principle, may consist of a combination of both member- and structure-level techniques. Details about the numerical implementation of the proposed procedure are reported, along with the summary of some relevant applications to RC frames representative of a wide class of buildings currently existing in South European Countries, such as Italy and Greece.

# 1. Introduction

The damages induced by recent earthquakes have dramatically highlighted that Reinforced Concrete (RC) buildings in earthquake-prone areas are generally characterized by medium-to-high seismic vulnerability [1]. Particularly, in Europe a significant part of those buildings have been realized after World War II and, hence, they have been designed according to codes and standards in force at that time, quite often without considering any seismic actions or, in some cases, taking them into account in a very simplistic way, far less consistent than the modern design approach provided by the codes currently in force in Europe [2].

The vulnerability of buildings depends on their so-called seismic "deficiency". More specifically, existing RC structures are affected by both local and global deficiencies, according to a possible classification available in the literature [3]. The former depend on poor detailing of single structural members or joints, inadequate sizing of cross sections or steel reinforcement, which make "capacity" of a single member. Conversely, the latter are typically due to lack in conceptual design or presence of irregularities (either in plan or in elevation) in the structural configuration, which result in an irregular distribution of seismic "demand" across the "primary" structural elements. Partial damage is generally accepted by the current design regulations for the "secondary" components which have been proven to be efficiently involved in the dynamic of the system [4].

Although demolition and reconstruction could be regarded as the most "efficient" solution for reducing the seismic vulnerability of the built stock, several reasons (among other things, dealing with economic, architectural, urbanistic aspects) rather drive owners towards preserving existing buildings. Therefore, seismic retrofitting is a widely considered solution, which is intended at reducing the vulnerability to the levels accepted by the current codes for newly designed structures. Specifically, retrofitting aims to fix the main weakness and deficiencies related to the seismic performance of the "as-built" structure by either strengthening deficient members or modifying the whole structure.

A widely accepted classification defines "member-level" (also called "local") and "structure-level" (also called "global") retrofit techniques [5]. Member-level techniques aim to enhance "capacity" of single members: a wide variety of "member-level" solutions are currently available in the market and include strengthening techniques as diverse as jacketing with concrete [6], steel [7] or fiber-reinforced polymer (FRP) sheets [8]. Conversely, structure-level techniques are intended at reducing "demand" on the existing building

by adding further substructures working in parallel with it: connecting RC shear walls [9] or steel bracing systems [10] with the existing members or introducing seismic isolators between superstructure and foundation are relevant examples of such techniques.

That said, it is clear that member- and structure-level techniques, considered on their own, represent two somehow "extreme" options to "enhance" the existing structures and they are not usually employed together; yet, they could suitably be combined with the aim to obtain "synergistic" effects [11]. However, no well-established rules are currently available for choosing the rational (not to say "optimal") combination of technical solutions belonging to the two aforementioned classes.

Moreover, in the current practice, as well as in many relevant scientific contributions on this topic [12], seismic retrofitting of RC frames is addressed as a merely technical problem. Apart from some pioneer contributions [13][14], in the Authors' best knowledge, no relevant study is currently available for approaching the selection of the most structurally efficient and cost-effective seismic retrofitting solution as an optimization problem.

Conversely, considerations about optimization (often restricted to the "economic" standpoint) are left to engineers and, hence, they are not part of a systematic and "objective" design approach. In fact, the so-called engineering judgment, a combination of "subjective" skills, such as intuition, experience, and common sense, is the main driver in designing retrofit interventions.

In this framework, the present paper proposes a more "objective" approach to select the "fittest" retrofitting solution obtained by combining structure and member-level interventions in the seismic retrofitting of existing RC framed structures. More specifically, it is based on a "Genetic Algorithm" (GA) [15], a meta-heuristic algorithm inspired to the Darwin's "evolution of species" [16] and the Mendel's "inheritance laws" [17], widely used for optimization problems.

In the authors' best knowledge, this is the first contribution to the scientific literature that targets seismic retrofitting by following a GA approach. Indeed, recent scientific contributions about the use of GA in seismic engineering have been restricted to the design of new structures [19]-[21]. It is worth highlighting that the purpose of the proposed procedure is to support engineering judgment (being far from the ambition to rule it out) in the challenging task of designing seismic retrofitting. Furthermore, multi-hazard scenarios, that has recently attracted the interest of the scientific community [22], are not considered in this study.

The paper is organized as follows: Section 1 proposes the general formulation of the problem, Section 2 provides the details about the implementation of a GA-based optimization procedure in the MATLAB environment and its relationships with seismic analyses carried out in OpenSEES [23], and Section 3 reports some relevant applications of the proposed procedure and the main conclusions of this research.

# 2. Conceptual formulation of the problem

Any seismic retrofit "strategy" has to be based on the Performance-Based Design principles [24]. Therefore, under the conceptual standpoint, it should lead to meeting the following inequality:

$$g_{LS} = C_{LS} - D_{LS} \geq 0 \quad \forall LS = 1 \dots n_{LS} \tag{1}$$

where $\boldsymbol{C_{LS}}$ is the Capacity of the structure at the Limit State (or Performance Level) and $\boldsymbol{D_{LS}}$ is the corresponding Demand at the same LS, for all the $n_{LS}$ Limit States of relevance for the structure under consideration [25]. The quantities in Eq. (1) can be defined in terms of either displacement for ductile mechanisms or forces for brittle mechanisms [26] (Fig. 1).


***Fig. 1:*** *Example of brittle mechanism (left); and ductile mechanism (right)*

Seismic displacement-based analyses are generally carried out with the aim to identify deficiencies and quantify the seismic vulnerability that can ideally be "measured" by the quantities in Eq. (1).

Old existing RC structures do not generally meet Eq. (1) and, hence, they need to be retrofitted. To this end, member-level techniques aim to increase the seismic capacity $C_{LS}$ of the structure by acting on the under-designed members, whereas structure-level techniques aim at reducing demand $D_{LS}$ on the existing buildings. Therefore, structural engineers are called to choose the "fittest" technical solution leading the existing structure to comply with Eq. (1).

In principle, the selection of the "best" retrofitting solution should be based upon Multi-Criteria Decision-Making (MCDM) procedures [27], which, however, do not aim at determining an "optimal" solution in an absolute mathematical sense, but they rather draw up a classification of the considered solutions, according to pre-established and discriminating criteria [28]. Such criteria could be based on both strictly quantitative measures, such as specific parameters related to the seismic response of the retrofitted structures or with the levels of reliability of its seismic performance, or qualitative measures, possibly related to either the users' opinion or aesthetical aspects of the final solutions.

This paper aims at formulating the seismic retrofitting of existing RC frames as a constrained optimization problem that can be mathematically written in the following form:

$$\mathrm{x}_{best} = argmin\,[eval(\mathrm{x_i})]\ \ with\ \ \mathrm{x_i} \in \Omega_f \subseteq S \tag{2}$$

where $\boldsymbol{x_i}$ is the vector of decision variables defining the generic retrofitting interventions, and $\boldsymbol{x_{best}}$ is the vector of the "optimized" variables with respect to the objective function $\boldsymbol{eval(x_i)}$. On the right-hand side of the Eq. (2), $\boldsymbol{\Omega_f}$ is the region including the structurally efficient solutions (namely, those for which $g_{LS} \geq 0$) within the whole search space $\boldsymbol{S}$. Specifically, two main Limit States dealing with the safety check at both Serviceability Limit State (in terms of Damage Limitation, SLD) and Ultimate Limit State (in terms of Life Safety, SLV) are considered herein [2]. The constraint of belonging to $\boldsymbol{\Omega_f}$ ensures that, for the "best" vector $\boldsymbol{x_{best}}$, the term $D_{LS}$ does not exceed the term $C_{LS}$.

The present work is bound to assuming the total cost of the intervention $\boldsymbol{C_{tot}(x_i)}$ as the objective function whose minimization leads to the cheapest seismic retrofitting solution among the ones that do not violate the inequality in Eq. (1). Although the objective function is simply represented by the initial cost the inclusion of costs deriving by the strengthening of foundation elements is also taken into account, which is not common in researches devoted to seismic retrofitting of RC frames.

Since no information about the convexity is explicitly known for the assumed objective function of Eq. (2), the cheapest solution cannot be obtained through the common analytical procedures based on the evaluation of derivatives and gradients. For the above-mentioned reason, the authors propose a GA-based procedure that looks for the "best" retrofitting solution.

# 3. Implementation of the Genetic Algorithm

The GA emulates the biological evolution of living beings. Specifically, each set of possible interventions is encoded in a chromosome: a mapping rule is established between phenotype (including the actual value of the relevant variables) and genotype (the conventional representation of the same decision variables in a well-defined code). An initial population of individuals (or chromosomes) is generated by considering both background knowledge about the problem under consideration and the randomness. Step by step, the GA produces solutions which are typically better adapted to the environment, encoded by the "fitness" function, used to rank each chromosome.

The evolutionary process goes on until some desired stop condition is reached. It is pursued through a peculiar algorithmic framework whose main components are the selection operators (parent selection and survivor selection) and the evolutionary stochastic operators (crossover and mutation). The crossover operator combines, in a probabilistic manner, pairs of "parent" individual in newly created pairs of "offspring" individual. The mutation operator, instead, randomly perturbs (locally in the strings) the offspring chromosomes by introducing some genetic features that were not present in the chromosomes of their parents.

The remaining part of this section describes in detail the steps of the procedure.

## 3.1 Chromosome definition and procedure starting

In the present implementation, two specific techniques are considered for the seismic retrofitting (Fig. 2):

- FRP jacketing of columns (as member-level technique);
- the introduction of concentric X-shaped steel bracings (as structure-level technique).

Based on this assumption, the chromosome of any "candidate" solution should include information describing a retrofitting intervention potentially consisting of both techniques. Specifically, the chromosome is structured by concatenating the set of variables representing both local and global interventions, respectively in the first part and in the second part of the vector $\boldsymbol{x}_i$. It is worth noting that the way of ordering columns and beam elements is part of the mapping genotype → phenotype.

***Fig. 2**: Example of local confinement (left); and concentric steel bracing (right)*

For the application described in this paper, the "sequence" of decision variables of the problem has been chosen consistently with the label assigned to each structural element, as shown in Fig. 3. Clearly, any other way of labeling the elements can be adopted, provided that the one-to-one "correspondence" between variables and structural elements is preserved.

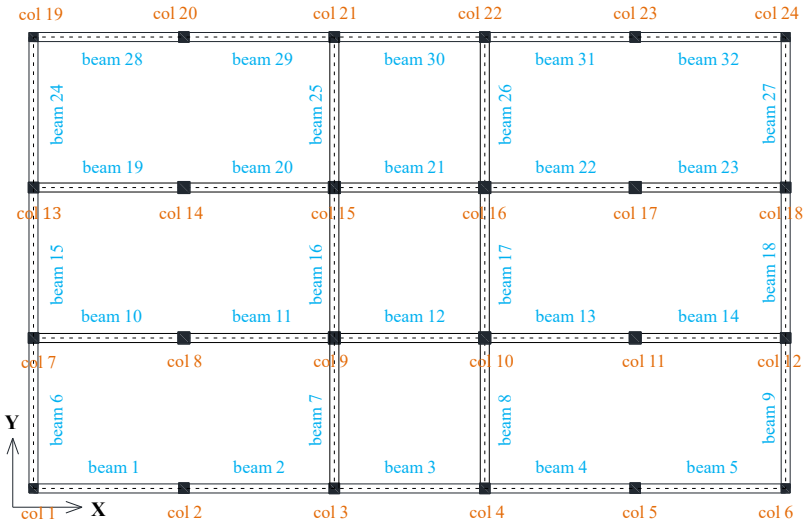


***Fig. 3**: Example of labels for columns and beams belonging to a regular structure*

The bracing systems, which could be placed across any bay "covered" by a beam, are considered to be present throughout the whole height of the frame with the aim to reduce the cardinality of the chromosome. Therefore, only the variables (e.g. the section of profiles) describing the bracings applied at the first story are needed, whereas the section at the upper storeys can be derived by applying a consistent design criterion (which currently consists of a force-based design approach).

In the first part of the chromosome, the decision variables (genes) are represented through an integer number (ranging between 0 and 3) encoding the number of FRP layers $n_{L,hk}$ possibly employed for confining

the h-th column at the k-th floor. Hence, in the first part of the genotype, a total of ***numCol*** variables is contained, where ***numCol*** is the number of column elements in the existing frame.

In the second part of the chromosome, each bracing system is described by an integer number (ranging between 0 and 7) which encodes the label of the steel section $ID_{sec,Nbt}$ adopted for realizing the diagonal bracing in correspondence of the $N_{bt}$-th beam. Hence, the second part consists of ***numBeam*** variables, ***numBeam*** being the number of beam elements in the structural model of the existing frame at the first floor (and, hence, the maximum number of bracing systems that can be actually installed). Fig. 4 depicts an example of decimal coding.

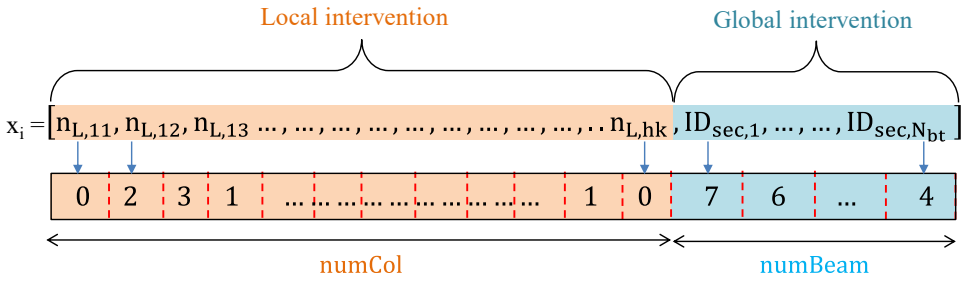


***Fig. 4****: Example of decimal genotype for encoding both local and global intervention*

As already seen, the proposed procedure starts by generating a population ***Pop*** of individuals (candidate solutions) in the form of a ***PopSize*** x $N_{var,tot}$ binary matrix, where $N_{var,tot}$ is the total number of variables in the chromosome given by the equation:

$$N_{var,tot} = numCol + numBeam \tag{3}$$

The proposed implementation employs a population with ***PopSize*** of 50 individuals, kept constant throughout the whole procedure. As for the initialization strategy, two different methods are combined. On the one hand, randomness is ensured by spreading a part $N_{rand}$ x $N_{var,tot}$ of the population uniformly over the search space (which can produce also poor-quality individuals). On the other hand, the background knowledge (heuristic) of the engineer (which is likely to produce "good-quality" individuals) is considered by concentrating the counterpart $N_{seed}$ x $N_{var,tot}$ of the population in the most promising regions (where more likely the admissible solutions will be) of the search space. In the current implementation $N_{rand}$ is equal to 20 and, hence, $N_{seed}$ is 30.

## 3.2 Finite Element modeling

Starting from the FE model of the as-built structure, the subroutine ***femodel*** reads the decimal matrix row by row and automatically modifies the model with the aim to include local and/or global interventions according to the information contained in the current i-th chromosome.

The data collected in the first part of the chromosome are employed for modifying the original (unconfined) stress-strain relationship describing the concrete behavior in each column. According to the uniaxial Kent-Scott-Park model [29], the effects of $n_{L,hk}$ layers of FRP strips are taken into account by increasing post-peak strength and ultimate strain: the original mechanical parameters describing the concrete behavior are duly modified to define the non-linear mechanical behavior of the confined concrete, as shown in Fig. 5.

Conversely, in the second part of the chromosome, the decision variables $ID_{sec,Nbt}$ point to a position in a commercial steel profile table containing a list of available commercial H-shaped profiles with their relevant geometric properties. The information collected in this part is employed for adding a new steel concentric bracing system to the FE model.

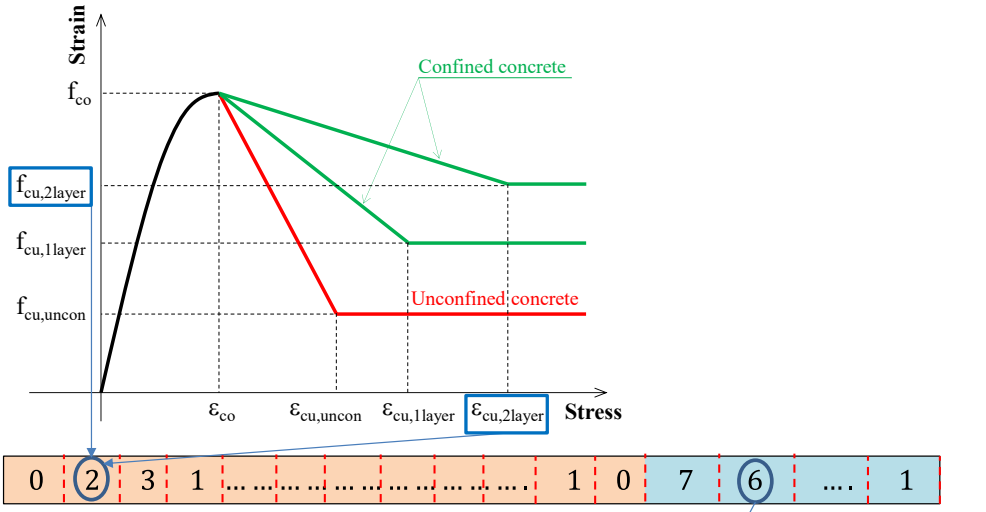


| LABEL | HEB | b [mm] | h [mm] | a [mm] | e [mm] | r [mm] | $A_1$ [cm²] |
|---|---|---|---|---|---|---|---|
| **1** | 100 | 100 | 100 | 6,0 | 10,0 | 12 | 26,04 |
| **2** | 120 | 120 | 120 | 6,5 | 11,0 | 12 | 34,01 |
| **3** | 140 | 140 | 140 | 7,0 | 12,0 | 12 | 42,96 |
| **4** | 160 | 160 | 160 | 8,0 | 13,0 | 15 | 54,25 |
| **5** | 180 | 180 | 180 | 8,5 | 14,0 | 15 | 65,25 |
| **6** | 200 | 200 | 200 | 9,0 | 15,0 | 18 | 78,08 |
| **7** | 220 | 220 | 220 | 9,5 | 16,0 | 18 | 91,04 |

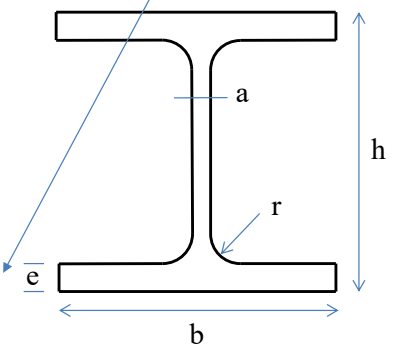


***Fig. 5****: Modification of the FE model according to the decision variables*

The following relationship is assumed in the current implementation between the section of steel members at the first level and the section of steel bracings at upper levels:

$$A_{k,des} = \frac{\sum_{j=k}^{nStor} h_j \cdot W_j}{\sum_{i=1}^{nStor} h_i \cdot W_i} \cdot A_1 \quad (4)$$

where $h_j$ represents the position in height of the j-th story with respect to the foundation level, ***nStor*** is the total number of stories, $W_j$ is the seismic mass of the j-th floor, $A_1$ is the area of the cross-section of the bracing elements at the first level and $A_{k,des}$ is the theoretical area of the cross-section required at the k-th floor. Alternative and more refined design approaches could be followed to determine the geometric properties of the bracings in the upper story based on those of the first one.

In the current implementation, a force-based spread plasticity element ("*nonlinearBeamColumn*") available in the OpenSEES' library is used to model the concentric steel bracings, while the "fiber section approach" is considered to take into account the inelasticity of steel [30]. Each bracing element is discretized into five H-shaped cross-sections located at the Gauss-Lobatto quadrature integration points: two integration points at the element edge and three in the middle (Fig. 6).

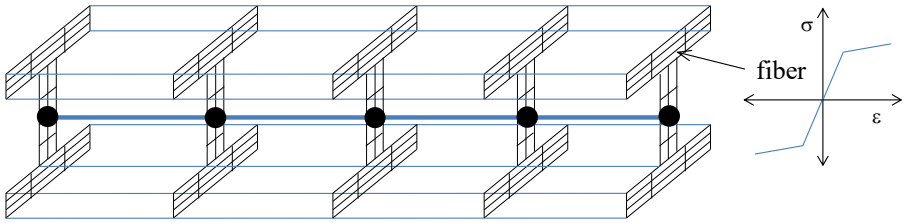


***Fig. 6****: Representation of integration points in the bracing members*

Moreover, since the concentric X-shaped steel bracing is modeled through four elements whose length is one half of the diagonal, an accidental eccentricity is assigned to the "middle point" (out of the plane where the bracing system lies) according to EN 1993-1-1 [31] for simulating the buckling effects in the compressed elements.

## 3.3 Seismic Analysis

Seismic analyses are required to "measure" the Capacity of the building (in both as-built and retrofitted configuration) and to compare it with the Demand according to the Eq. (1). Among the several tools available to carry out such seismic simulation, the choice of the authors fell on OpenSEES, an open-source program that

can run any advanced - linear or nonlinear, static or dynamic - analysis procedure. However, in the current implementation, the ***seismic*** subroutine (for the i-th solution) executes a "pushover" analyses of the "updated" FE model (which includes the retrofitting interventions) to estimate the performance of the strengthened structure under the expected seismic actions.

Lateral loads distribution with an inverted triangle shape, particularly fit for regular structures (whose response is clearly dominated by the first mode of vibration) is considered; a target displacement $\Delta_{maxU}$ equal to 0.03*$H_{tot}$ is sought; while the displacement step of the incremental analysis is set to 1% of the maximum displacement. For the sake of brevity, only one pattern horizontal actions is considered in this work (Fig. 7), but further patterns (e.g. horizontal forces proportional to the floor masses) could be added at the only cost of a more time-consuming FE analysis.

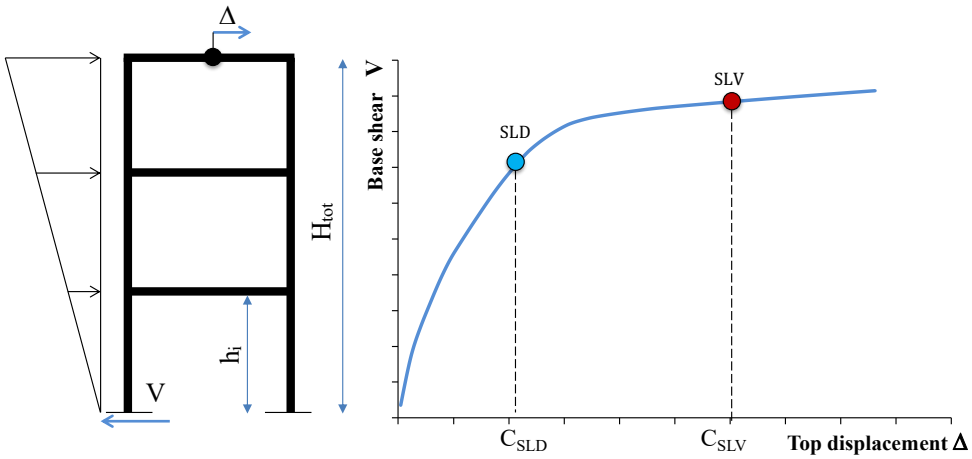


***Fig.** 7: Typical trend of a pushover curve*

Moreover, the seismic response of the structures is simulated along two orthogonal directions, also considering the possible inversion of the seismic action. Hence, for each candidate solution 4 pushover analyses are executed: X towards positive, X towards negative, Y towards positive and Y towards negative.

Since the GA works with a population of independent retrofitting solutions (whose FE models do not depend on each other), it is worth noticing that this stage can be executed completely in parallel, hence fully exploiting the potential of any multi-core processor.

## 3.4 Post-Processing

### 2.4.1 Evaluation of objective functions

The subroutine ***postprocess*** aims at determining, among the others, the costs of the i-th retrofit solution. To this end, the proposed procedure takes into account the actual initial cost $C_{tot}$ of the intervention, defined as follows:

$$C_{tot}(\mathrm{x_i}) = C_{loc}(\mathrm{x_i}) + C_{glob}(\mathrm{x_i}) + C_{found}(\mathrm{x_i}) \tag{5}$$

where $C_{loc}$ is the cost of local strengthening of columns through FRP layers, $C_{glob}$ is the cost of global intervention realized by installing a set of steel bracing systems, and $C_{found}$ is the cost of the possible strengthening of the existing foundation system. The first term is calculated according to the following relationship:

$$C_{loc}(\mathrm{x_i}) = \sum_{col=1}^{numCol} \left[ C_{dem,loc}{}_{col}(\mathrm{x_i}) + C_{rest,loc}{}_{col}(\mathrm{x_i}) + C_{FRP,layer}{}_{col}(\mathrm{x_i}) \right] \tag{6}$$

where the term $C_{dem,loc}$ refers to the cost of demolition of the existing partitions adjoining the column, the term $C_{rest,loc}$ is the cost of reconstruction of the masonry once the local intervention is completed, and the term $C_{FRP,layer}$ represents the cost of the Fiber Reinforced Polymeric material and its application in layers to confine the corresponding columns. These terms are positive if and only if the decision variable corresponding to the *col-th* column in the first part of the vector $x_i$ has a non-zero value. Likewise, the cost of global intervention is calculated through the following summation:

$$C_{glob}(\mathrm{x_i}) = \sum_{beam=1}^{numBeam} \left[ C_{dem,glob}{}_{beam}(\mathrm{x_i}) + C_{rest,glob}{}_{beam}(\mathrm{x_i}) + C_{SteelB}{}_{beam}(\mathrm{x_i}) \right] \tag{7}$$

where the term $C_{dem,glob}$ refers to the cost of demolition of the existing partitions under the corresponding beam, the term $C_{rest,glob}$ is the cost of reconstruction of the partition once the global intervention is completed, and the term $C_{SteelB}$ represents the cost of steel diagonal elements and their installation as a concentric bracing system. It is worth highlighting that both $C_{loc}$ and $C_{glob}$ do not depend on the outcome of seismic analyses. The unit costs for the operations of demolition and restoration of masonry are respectively 8.50 €/m$^2$ and 47.50 €/m$^2$. With regard the costs of the FRP wrap a distinction is made depending on whether it is the first or the next layers: in the former case, the unit cost is 207 €/m$^2$ while in the latter it is 168 €/m$^2$. On the other hand, the unit cost of steel members is assumed equal to 3.05 €/kg.

Moreover, Eq. (5) also includes the cost $C_{found}$ of the possible strengthening of the existing foundation system (supposed to be made with micro-piles) needed to respond to the increase in vertical and horizontal reactions at the base of the structure. The number of micro piles actually needed is obtained by considering that the seismic actions on the strengthened frame can result in higher axial forces at the bottom of each column, with respect to the gravitational loads only. To this end, the ***postprocess*** subroutine compares the maximum axial forces before and after the retrofit intervention: the number of micro-piles required at the base of the i-th column is proportional to the difference in the axial forces $\Delta N_i$ according to the following ratio:

$$N_{mp,col} = \frac{\Delta N_{col}(\mathrm{x_i})}{Q_{lim,mp}} \tag{8}$$

where $Q_{lim,mp}$ is the bearing capacity of the micro-pile (set to 460 kN), uniquely determined on the basis of its diameter $D_{mp}$ (120 mm), length $L_{mp}$ (10 m), construction type and ideally related to the geotechnical properties of the subsoil. Hence, the cost $C_{found}$ stems out from the relationship shown below:

$$C_{found}(\mathrm{x_i}) = \sum_{col=1}^{numCol} \left[N_{mp,col} \cdot \left(C_{micropile} + C_{excav} + C_{concrete}\right)\right] \tag{9}$$

where $C_{micropile}$ is the unit cost for the installation of a single micro-pile (including the shuttering and the longitudinal reinforcing steel profile) equal to 1058 €/microp, $C_{excav}$ is the excavation unit cost equal to 144 €/m$^3$, and $C_{concrete}$ is the unit cost of concrete needed to build the plinth equal to 122 €/m$^3$. However, the readers can refer to any price list of public works for the choice of the unit costs.

### 2.4.2 Evaluation of constraints

Since both economic viability and technical effectiveness are considered as discriminating criteria for the final choice of the decision-maker, the outcomes of the seismic analysis are interpreted to check the performance constraints for each candidate solutions. In accordance with Eq. (1), the subroutine ***postprocess*** evaluates the Limit State function $g_{LS}$. It's worth saying that in the author's preliminary proposal both $C_{LS}$ and $D_{LS}$ are defined only in terms of displacement (for ductile mechanisms).

On the one hand, inter-story demand drifts $\delta_D$ are considered herein as the seismic response parameter to find the pushover step at which the Limit State Capacity is achieved. The structure is supposed to reach the Limit State Capacity at the exceeding of certain thresholds value. To this end, the drift capacity $\delta_{C,SLV}$ of the

column elements at SLV is defined in terms of chord rotation at collapse conditions $\boldsymbol{\theta_{um}}$ obtained by the empirical formulation [32]:

$$\delta_{C,SLV} = \theta_{um} = \frac{1}{\gamma_{el}} \cdot 0.016 \cdot (0.3^{\nu}) \cdot \left[\frac{max(0.01;\omega')}{max(0.01;\omega)} \cdot f_c\right]^{0.225} \cdot \left(\frac{L_v}{h_{sec}}\right)^{0.35} \cdot 25^{\left(\alpha \cdot \rho_{sx} \cdot \frac{f_{yw}}{f_c}\right)} \cdot (1.25^{100-\rho_d}) \quad (10)$$

where h is the depth of cross-section, $L_v$ is the ratio moment/shear at the end section, α is the confinement effectiveness factor, ω (ω') is the mechanical reinforcement ratio of the tension (compression) longitudinal reinforcement, ν is the dimensionless axial force, $\rho_d$ is the steel ratio of diagonal reinforcement, $f_c$ and $f_{yw}$ are the concrete compressive strength and the stirrup yield strength, respectively. Similarly, the drift capacity $\boldsymbol{\delta_{C,SLD}}$ of the column elements at SLD is defined in terms of chord rotation at yielding $\boldsymbol{\theta_y}$ conditions:

$$\delta_{C,SLD} = \theta_y = \left(\theta_{um} - \theta_{um}^{pl}\right) \quad (11)$$

where $\theta_{um}^{pl}$ is given by thee following equation:

$$\theta_{um}^{pl} = \frac{1}{\gamma_{el}} \cdot 0.0145 \cdot (0.25^{\nu}) \cdot \left[\frac{max(0.01;\omega')}{max(0.01;\omega)} \cdot f_c\right]^{0.35} \cdot f_c^{0.25} \cdot \left(\frac{L_v}{h_{sec}}\right)^{0.35} \cdot 25^{\left(\alpha \cdot \rho_{sx} \cdot \frac{f_{yw}}{f_c}\right)} \cdot (1{,}275^{100-\rho_d}) \quad (12)$$

Moreover, the assessment of seismic performances takes into account the biaxial response of the structure by mean of a nonlinear interaction domain of the drifts (along both X and Y axis):

$$C_{LS}(\mathrm{x_i}) \Leftarrow \left[\left(\frac{\delta_D}{\delta_{C,LS}}\right)_X^{1.5} + \left(\frac{\delta_D}{\delta_{C,LS}}\right)_Y^{1.5} = 1\right] \quad (13)$$

On the other hand, the procedure includes the N2-Method [33] to estimate the maximum expected displacement Demand $\boldsymbol{D_{LS}}$. For determining the so-called "*performance point*", the subroutine ***postprocess*** converts the pushover curve into a Capacity Spectrum represented in the Acceleration-Displacement-Response-Spectra (ADRS) format characterized by spectral acceleration $\boldsymbol{S_{ae}(T)}$ on the y-axis and spectral displacement $\boldsymbol{S_{de}(T)}$ on the x-axis, being $\boldsymbol{T}$ the period of vibration. The $\boldsymbol{V\text{-}\Delta}$ curve of the multi-degrees-of-freedom (MDoF) system is converted into a $\boldsymbol{V^*\text{-}\Delta^*}$ curve representative of the behavior of an equivalent single-degree-of-freedom (SDoF) system through the modal participation factor $\boldsymbol{\Gamma}$. The $\boldsymbol{V^*\text{-}\Delta^*}$ curve is then simplified to obtain a bilinear relationship whose main parameters are: the yielding displacement $\boldsymbol{\Delta_y^*}$, the ultimate displacement $\boldsymbol{\Delta_u^*}$, and the shear strength $\boldsymbol{V_y^*}$ (Fig. 8).

Hence, the subroutine calculates the inelastic displacement demand for the equivalent SDoF $\boldsymbol{S^*_{d,max}}$ as the intersection point between the Capacity Spectrum and the Inelastic Demand Response Spectrum (IDRS). The

latter is obtained starting from the Elastic Demand Response Spectrum (EDRS), scaled by the reduction factor $R_\mu^*$ of the SDoF [34].

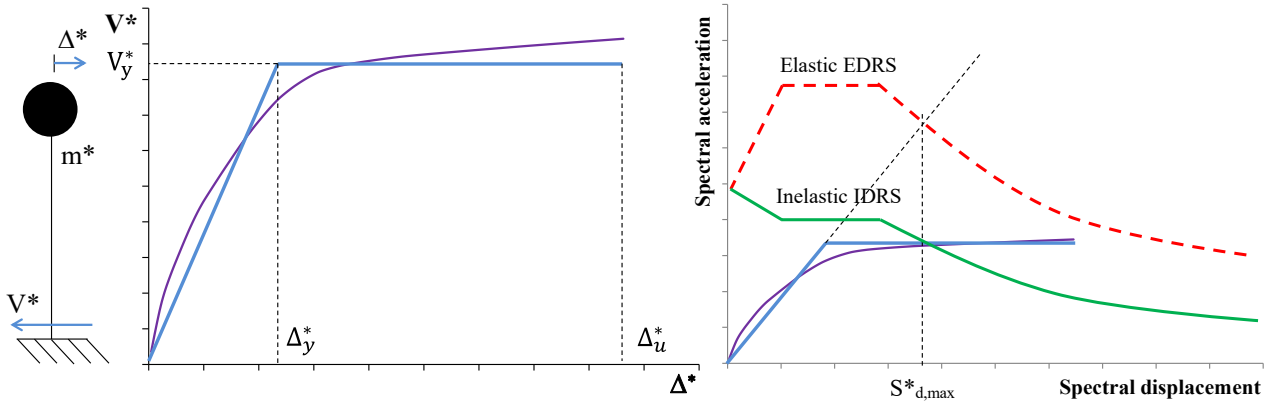


***Fig. 8**: Evaluation of seismic displacement Demand via N2 Method*

As the last step of N2-Method, the subroutine converts the inelastic displacement demand $S^*_{d,max}$ of the SDoF system to the inelastic displacement demand $D_{LS,i}$ of the original MDoF system according to the relationship below:

$$D_{LS}(\mathrm{x_i}) = \Gamma \cdot S^*_{d,max} \tag{14}$$

Since 2 relevant Limit States and 4 lateral load patterns are considered, a total of 8 values of displacement Demand and Capacity are determined. A candidate solution is considered belonging to the feasible region $\Omega_f$ if and only if the minimum difference among all the 8 combinations meets the following condition:

$$\mathrm{x_i} \in \Omega_f \subseteq S \quad if \min_{dir_j}\left[\min_{LS}\left(C_{LS}(\mathrm{x_i}) - D_{LS,i}(\mathrm{x_i})\right)\right]_j \geq 0 \tag{15}$$

where $\mathrm{LS} \in \{\mathrm{SLD}, \mathrm{SLV}\}$ and $\mathrm{dir_j} \in \{\mathrm{X+}, \mathrm{X-}, \mathrm{Y+}, \mathrm{Y-}\}$. Moreover, since the GA is directly applicable only to an unconstrained optimization problem, it is necessary to keep the solutions in the feasible region $\Omega_f$. Several methods have been proposed in the past for handling constraints [35]. The proposed procedure relies on an additive penalty term $p(x_i)$ consistent with the most widely adopted methods followed among the GA community and defined as follow:

$$p(\mathrm{x_i}) = \begin{cases} 0 & if\ \mathrm{x_i} \in \Omega_f \\ \beta \cdot C_{tot}(\mathrm{x_i}) & if\ \mathrm{x_i} \notin \Omega_f \end{cases} \tag{16}$$

More specifically, a kind of "Death Penalty Function" [36] is employed: if no violation occurs the penalty term will be zero, otherwise a high penalty term will be added to the cost so that the search is pushed back towards to the feasible region. Therefore, the new objective function $eval(x_i)$ to minimize is defined below:

$$eval(\mathrm{x_i}) = \begin{cases} C_{tot}(\mathrm{x_i}) & if\ \mathrm{x_i} \in \Omega_f \\ (1+\beta)\cdot C_{tot}(\mathrm{x_i}) & if\ \mathrm{x_i} \notin \Omega_f \end{cases} \quad (17)$$

where the factor β is chosen >> 1. Very low values may not produce the penalizing effect required for solving the constrained problem. Therefore, in light of several attempts, it's author's opinion that a value of $10^3$ is reasonably enough to penalize the technically unfeasible individuals.

## 3.5 Fitness function

The transformation objective function → fitness is not a trivial operation. The ***mapping*** subroutine employs a proportional fitness assignment [37]. In other words, the fitness of each individual is computed as its raw performance relative to the whole population, according to the equation:

$$F(x_i) = \frac{\min\limits_{i=1\ldots PopSize}[eval(x_i)]}{eval(x_i)} \quad (18)$$

Therefore, it is chosen as a real-valued and monotonic function of the objective function, ranging within the interval [0;1]. The monotonicity assures that fitness always improves with decreasing values of the objective: it is generally smaller than 1, as the unit value corresponds only to the "best" individual.

In the current proposal, once the ***PopSize*** chromosomes are ranked from lowest to highest fitness value, the worst individuals (retrofitting solutions that either have a very high cost or violate the constraints) are replaced with new ones. The number ***PopDisc*** of discarded chromosomes is equal to 0.95****PopSize***. This assumption assures that at least 5% of the population survives in the next generation.

## 3.6 Selection

Since GA imitates the human being's way of reproduction, the first operator involved in the evolution process selects a couple of "parents". The selection must conform to the basic idea of the "survival of the fittest" principle by giving a higher probability of recombination to individuals characterized by higher fitness. Such a probability is herein determined according to the following equation:

$$prob(x_i) = \frac{F(x_i)}{\sum_{i=1}^{PopSize} F(x_i)} \quad (19)$$

The ***selection*** subroutine employs the so-called "*roulette-wheel*" [38]: the circular sections of the wheel are not all the same but they are marked proportionally to the probability of survival of each individual, as shown in Fig. 9:

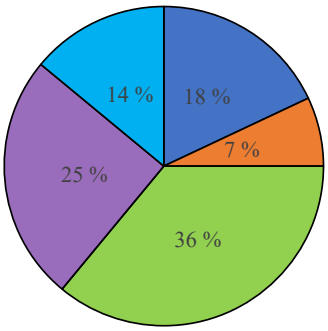


| Individual | chromosome $x_i$ | prob ($x_i$) | cumprob ($x_i$) |
|---|---|---|---|
| #1 | 2 0 3 1 2 1 0 1 3 3 1 2 3 1 4 6 0 5 3 0 4 0 7 | 0.18 | 0.18 |
| #2 | 1 1 2 1 0 1 3 0 3 2 1 2 2 0 3 0 2 1 3 1 4 2 7 | 0.07 | 0.25 |
| #3 | 1 0 0 1 1 1 2 2 1 0 2 1 0 3 7 4 0 3 5 2 3 1 5 | 0.36 | 0.61 |
| #4 | 0 2 1 3 3 2 1 3 0 2 3 2 2 0 3 0 3 1 3 1 4 2 7 | 0.25 | 0.86 |
| #5 | 3 3 3 2 0 3 1 0 2 3 1 3 2 1 5 5 0 4 6 5 1 0 0 | 0.14 | 1.00 |

***Fig. 9****: Working principle of roulette wheel selection rule*

According to this rule, a random number in the range [0; 1] is generated. Starting from the top of the list, the first chromosome with a cumulative probability higher than the random number is selected. For instance, if the random number is r = 0.57, then chromosome #3 in Fig. 9 is selected as parent because $0.25 < r \leq 0.61$. The number of drawn parents is equal to the number ***PopDisc*** of individuals discarded in the previous population in order to keep constant the number of individuals in the population.

This "soft" selection makes it possible to proliferate the genetic material contained in any chromosome, even the worst one, with chances depending precisely on its fitness. In this way, even the poorly-fitted individuals retain non-zero chance to become a parent and transmit their genetic material to the future generations.

## 3.7 Crossover

The working principle of the ***crossover*** subroutine implemented in the proposed algorithm is shown in Fig. 10 and Fig. 11: it is a sort of uniform crossover [39]. As can be seen, a crossover "mask" is created at random. The crossover "mask" consists of as many bits as the total number of traits (delimited with the dashed lines shown in Fig. 10) to be "exchanged". Therefore, the crossover operator "mixes" the genetic information of the two parents contained between traits of different lengths. In the current implementation, in the first part of the chromosome (which encodes the local interventions), each trait involves a number of decision variables equal to the number of columns belonging to a single storey of the building. In the second part of the

chromosome (which encodes the global intervention), instead, the traits group beams united by a symmetry criterion with respect to the X-axis or the Y-axis. Clearly, the choice of the traits in the second part of the chromosome becomes meaningless for irregular (i.e. asymmetrical) structures that, at least for now, have not been studied.

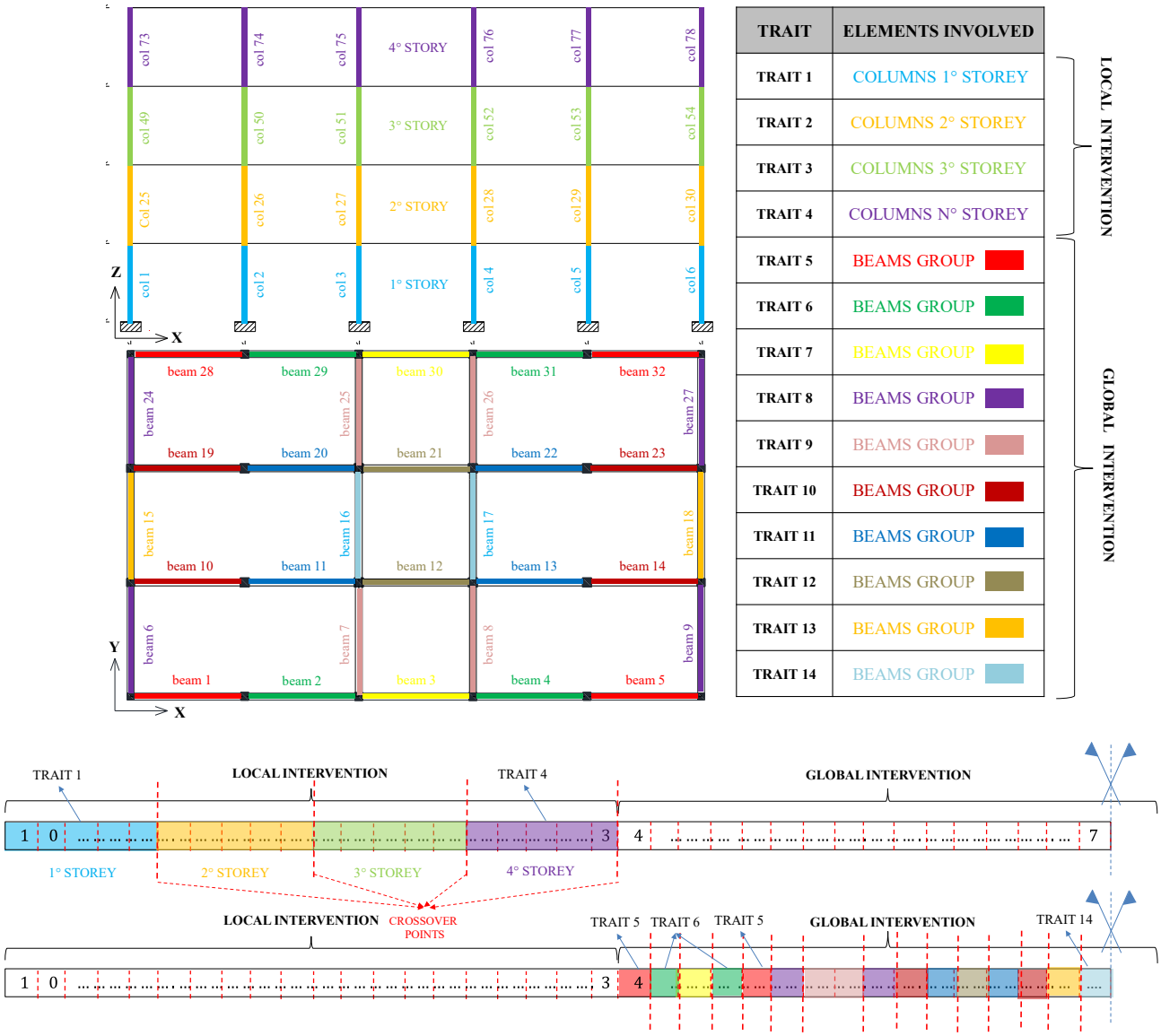


***Fig. 10**: Definition of the length of the traits to be exchanged and corresponding crossover points*

The bits randomly generated in the mask indicate which genes should contribute to the offspring's genotype: the offspring 1 ($O_1$) is produced by taking the gene from parent 1 ($P_1$) if the corresponding bit in the mask is 1 or, conversely, by taking the gene from parent 2 ($P_2$) if the bit in the mask is 0. The offspring 2 ($O_2$) is simply created by swapping the bit in the mask.

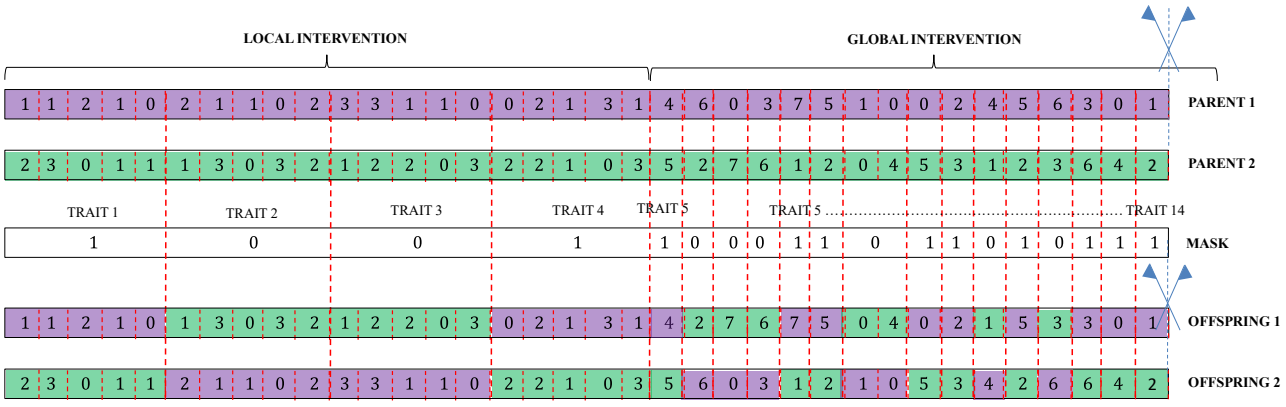


***Fig. 11**: Working principle of the proposed crossover operator*

## 3.8 Mutation

The mutation is the only way to recover valuable genetic material that may be lost because of the repeated use of the crossover operator. In fact, it may easily happen that offspring do not contain some information that might be present in the desired solution, but that genetic information is present in very poorly "fitted" individual, rarely selected for recombination. Under the conceptual standpoint, ***mutation*** subroutine aims at creating points in the neighbourhood of the current solution, thereby achieving a local "exploration" of the design space. It no longer acts at the traits' level: it modifies few, randomly selected, variables of the chromosome. In the present work, the number of mutations $N_{mut}$ occurring in an offspring is calculated according to the equation:

$$N_{mut} = \lfloor \mu_{mut}(numGen) \cdot N_{var,lot} \rfloor \tag{20}$$

where $\mu_{mut}$ is a problem-dependent parameter which plays an important role in the GA: if it's too high the population will never stabilize; too low and the algorithm will not be able to escape from local optima. As can be seen, $\mu_{mut}$ is chosen as a function of the number of generations ***numGen***:

$$\mu_{mut} = \mu_{mut,1} + \frac{numGen}{maxGen} \cdot \mu_{mut,1} \tag{21}$$

where $\mu_{mut,1}$ is set to 0.05. This "dynamic" genetic property is chosen to increase the algorithm's freedom to search outside the current region of variable space and to improve its ability to "escape" from local optima over the evolution time.

That said, a random number generator creates $N_{mut}$ integers (which range between 1 and $N_{var,tot}$) that correspond to the column positions of the decision variables to be changed in the mutated offspring ($O_{M1}$). At the same time, another random number generator provides, for the randomly selected variables, the "magnitude" of the mutations: it generates relative numbers belonging to the range [-3; 0] and to the range [-7; 0], depending on whether the variable is in the first or in the second part of the chromosome, respectively. The mutated variables are nothing but the algebraic sum of the previous values of the variables and the magnitude of the mutation, with the lower limit of such difference equal to zero (because the variables cannot be negative). The choice to generate negative "magnitudes" is due to the finding that the problem aims to minimize the value assumed by the variables describing the generic seismic retrofitting intervention. In fact, in general terms can be stated that as the value of these variables increases, the search moves away from the minimum cost solution. The working principle is shown in Fig. 12.

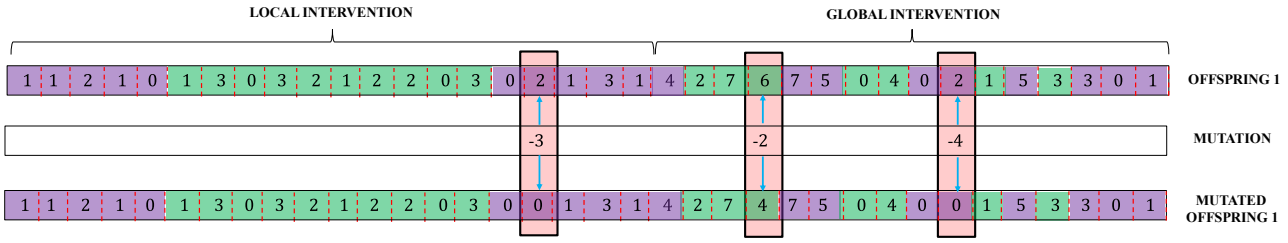


***Fig. 12**: Working principle of the proposed mutation operator*

The trio ***selection-crossover-mutation*** keeps running until the desired number of offspring are created to replace the ***PopDisc*** discarded individuals: in this way, the size of the population is restored to ***PopSize***.

# 4. Applications

## 4.1 Description of instances and test scenarios

The actual potential of the proposed optimization procedure can be well outlined by considering the preliminary example applications reported in this section. The applications concern a structure obtained through simulated design according to the practices and techniques in force in Italy during the 1970s. The structure has a very simple construction typology, regular in plan and in elevation. It is composed of four stories and the plan is characterized by a long side, short side and an inter-story height respectively equal to 25.00 m, 15.00 m, and 3.50 m, as shown in Fig. 13.

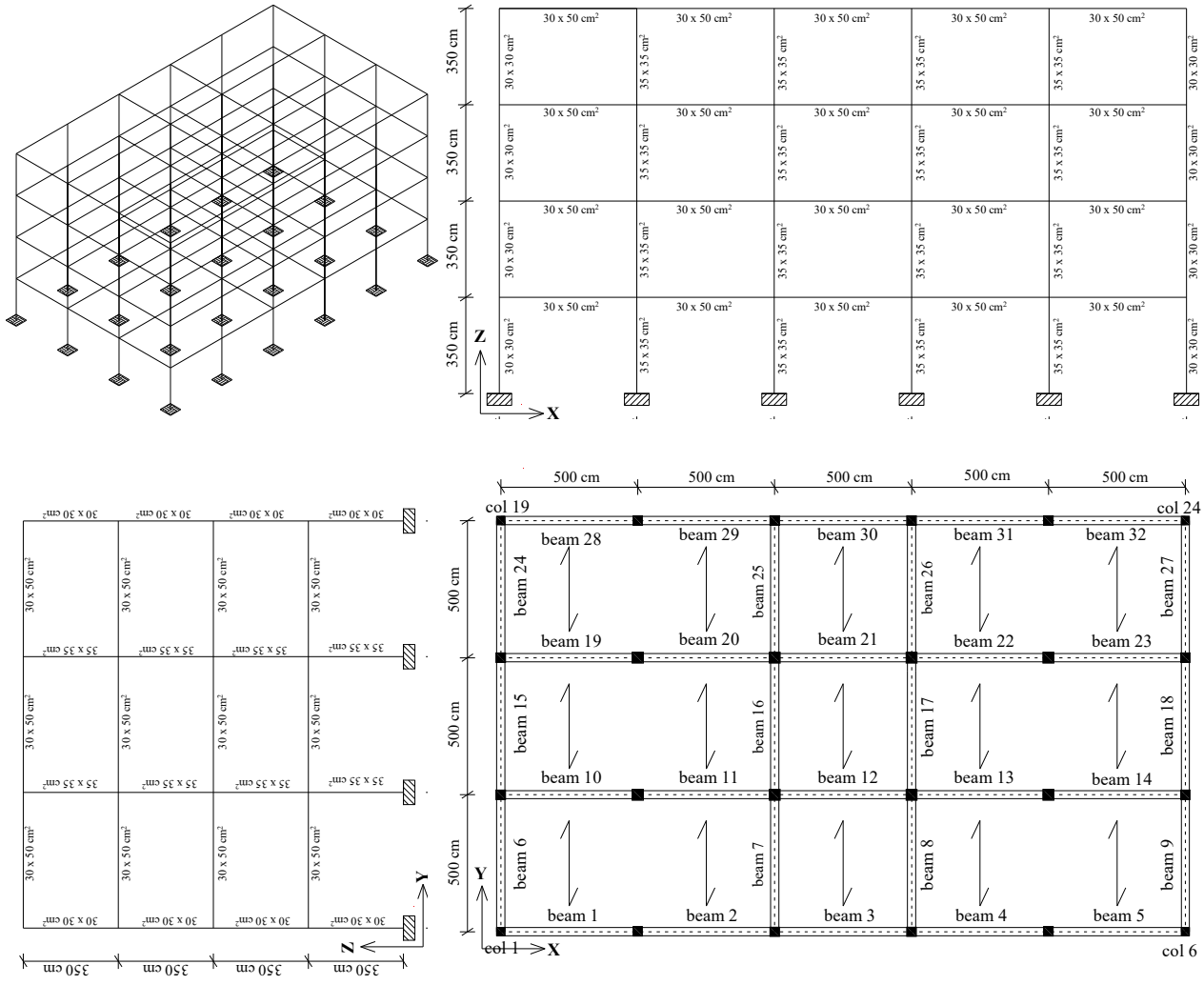


***Fig. 13**: Geometry of the existing structure under consideration*

A global coordinate system is used: the global Z-axis is the vertical direction of the structure, the global Y-axis is orthogonal to the horizontal plane, representing the transverse direction, while the global X-axis is denoted as the longitudinal direction.

The 3D view, the plan configuration, the elevation configurations of the structure both in the <ZX> plane and in the <ZY> plane, and the cross-section of the RC elements are shown in Fig. 13. The total number of columns ***numCol*** is equal to 96, while the number of the beam on the first-floor ***numBeam*** is 32. The analysis of loads, carried out for a square meter of the floor, has led to the following results: the permanent load is $\boldsymbol{G}$=5.00 kN/m$^2$ and the live load is $\boldsymbol{Q}$=2.00 kN/m$^2$. Gravity loads are applied to an effective area of 375 m$^2$. The seismic mass of the first three floors is $\boldsymbol{W_1} = \boldsymbol{W_2} = \boldsymbol{W_3}$ = 3540 kN, while the seismic mass on the fourth floor is $\boldsymbol{W_4}$ = 2940 kN.

The uniaxial Kent-Scott-Park model [29] with degraded linear unloading/reloading stiffness and no tensile strength is assumed for modeling the behavior of concrete and the effect of FRP confinement. Reference is made to a resistance class C20/25 where the first number means the cylindrical resistance $\boldsymbol{f_{ck}}$, while the second number indicates the cubic resistance $\boldsymbol{R_{ck}}$. A bilinear stress-strain curve is adopted for describing the elastic-plastic behavior of steel: the modulus of elasticity of steel is chosen equal to 210 GPa and the yield stress $F_y$ is 220 MPa.

The cross-section is discretized into fibers which comply with beam kinematics and each follows its own constitutive stress-strain response, the integration of which defines the stress resultant force-deformation response at a beam-column sample point. More specifically, the rectangular R.C. sections are composed of patches (groups of fibers): 4 cover concrete patches, 1 core concrete patch and 3 reinforcing layers of longitudinal rebars (top, bottom, and intermediate skin reinforcement layers), as shown in Fig. 14.

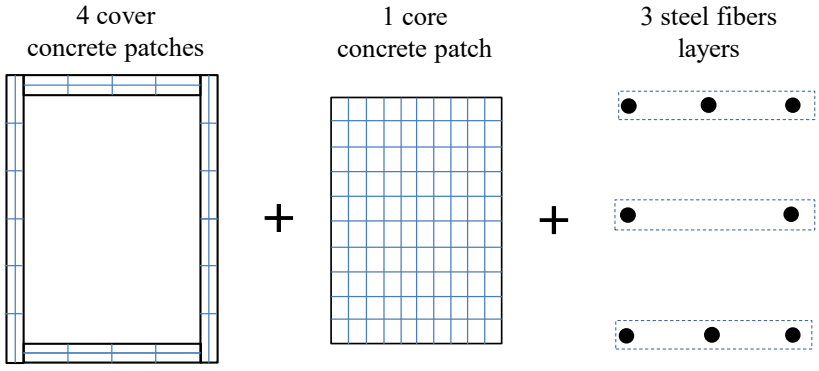


***Fig. 14****: Fiber section approach for the RC sections*

The core concrete patch is considered to be not confined by the transversal stirrups (due to their wide spacing) and it is discretized into 100 fibers. "*BeamWithHinges*" command is selected from OpenSEES library to construct a force-based nonlinear element: the plasticity is assigned at the end element in the so-called "*plastic-hinges*" region with a finite length $\boldsymbol{L_p}$, while the central part of the beam is simulated by a linear elastic element as shown in Fig. 15.

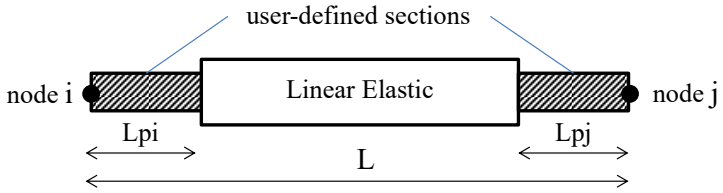


***Fig. 15**: Finite length hinge approach for RC members*

In the present work, the plastic hinge length $\boldsymbol{L_p}$ is chosen to be equal to the cross-section's height of the element. The floor, which is one of the most important elements for distribution of seismic actions, has been schematized with diagonals members made of a linear elastic material (with Young Modulus $\boldsymbol{E}$) because it cannot be considered infinitely rigid in its plane. To this end, truss elastic elements hinged at the ends are used. In the present work, the axial stiffness of diagonal truss is based on a reliable and widespread formula available in the literature and proposed by Yettram and Hussain [40].

The whole frame is assumed to have rigid joints for simulating beam-to-column connections. Foundation is not simulated, but fixed supports are considered. Non-structural elements are not included in the FE model. Moreover, the existing structure is assumed to be built in the municipalities characterized by Elastic Demand Response Spectra with a high severity level (Fig. 16 – Fig. 17), namely L'Aquila and Lioni, in central and southern Italy, respectively. Both the SLV and SLD Limit States are considered.

Fig. 16 and Fig. 17 depict both the Capacity Spectrum, which describes the nonlinear behavior of the as-built structure and the Elastic Demand Spectra, representative of the seismic input. The tables on the right, whereas, collect the difference between Capacity and Demand (in terms of displacement) for each lateral load patterns and Limit States considered.

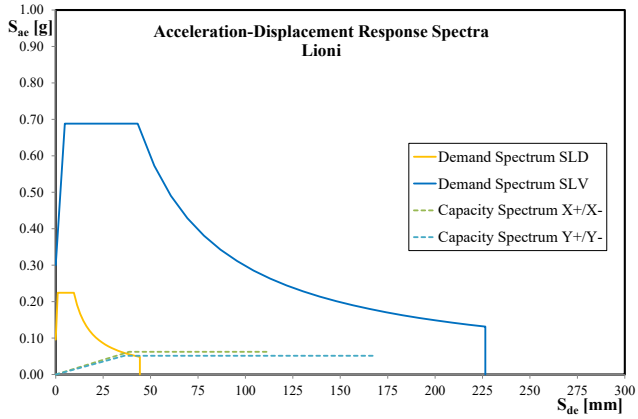


| | SLD $g_{LS}$ [mm] | SLV $g_{LS}$ [mm] |
|---|---|---|
| **Pushover X+** | 3.1 | -31.8 |
| **Pushover X-** | 3.1 | -31.8 |
| **Pushover Y+** | -0.1 | 32.1 |
| **Pushover Y-** | -0.1 | 32.1 |

***Fig. 16**: EDRS for Lioni (left); and quantitative starting condition (right)*

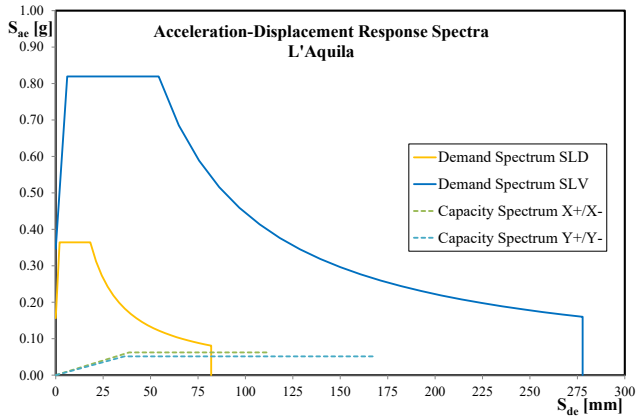


| | SLD $g_{LS}$ [mm] | SLV $g_{LS}$ [mm] |
|---|---|---|
| **Pushover X+** | -46.8 | -105.4 |
| **Pushover X-** | -46.8 | -105.4 |
| **Pushover Y+** | -53.2 | -46.1 |
| **Pushover Y-** | -53.2 | -46.1 |

***Fig. 17**: EDRS for L'Aquila (left); and quantitative starting condition (right)*

As can be seen, the structure in both cases is characterized by a significant vulnerability and, hence, requires a seismic retrofit intervention. The total number of decision variables (describing the generic retrofit intervention) to be optimized in the example is 128 (Fig. 18): 96 "member-level" variables (24 columns for each floor), plus 32 "structure-level" variables (20 beams in X-direction and 12 in the Y-direction). Therefore, the entire search space consists of $4^{96} \cdot 8^{32} = 4.9 \cdot 10^{86}$ candidate solutions.

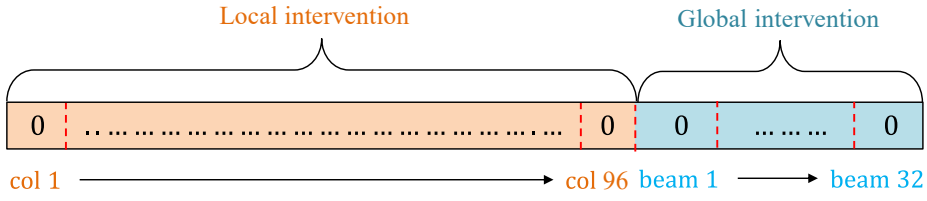


***Fig. 18**: Decimal genotype which encodes the as-built configuration and total number of variables*

In this case, the "exhaustive" search [41] (also called "brute force" search) cannot be used because exploring all possible solutions would take a very long CPU time (to perform $4*4.9*10^{86}$ pushover analyses). Hence, the GA-based proposed procedure has been applied to search for the "best" retrofit solution, from both economic and technical standpoints, because of the GA's ability of exploring the search space in parallel through the

generation of a reasonably limited number of candidate solutions (which may need the execution of at most 4 · 50 · 200 = 40000 pushover analyses). The applications have been carried out using the following hardware and software: Windows 10 Professional 64 bit, Notebook with 16 GB of RAM; Intel® Core™ i7-8750H CPU with 2.20 GHz, OpenSEES Version 2.5.0, and MATLAB Version R2018b. Since the initial population is based also on randomness which, in turn, results in different optimization outcomes, 5 runs of the GA-based procedure have been performed. The five curves of the cost's evolution are shown in Fig. 19 and Fig. 20, respectively for the cases of Lioni and L'Aquila.

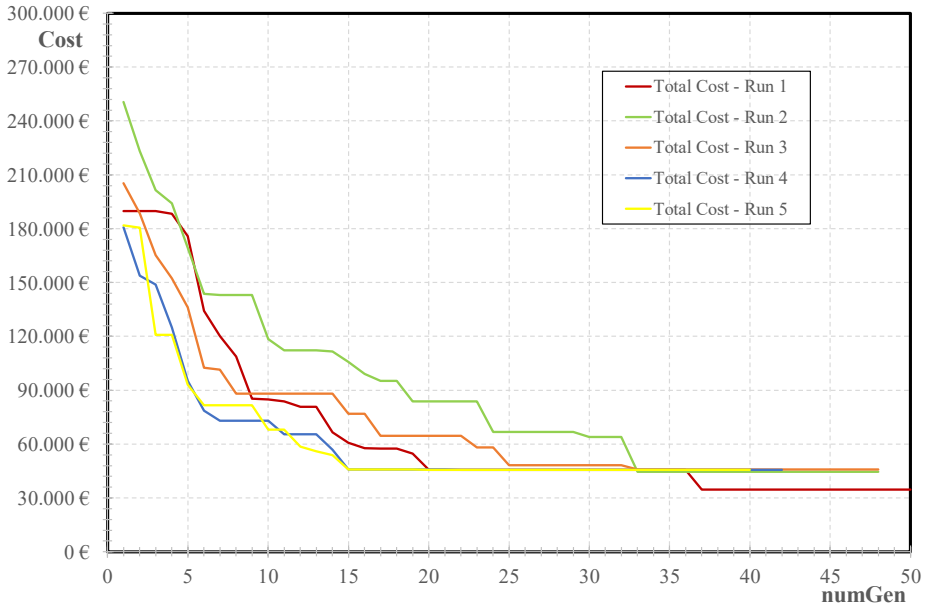


***Fig. 19**: Total cost function's evolution for several runs (case of Lioni)*

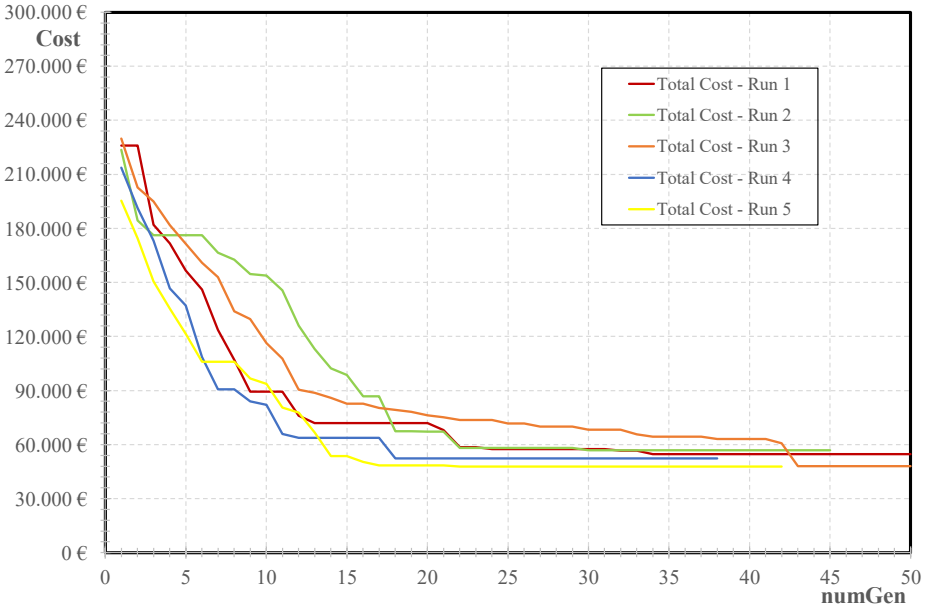


***Fig. 20**: Total cost function's evolution for several runs (case of L'Aquila)*

Fig. 21 and Fig. 22 depict only the results of the run that has produced the "cheapest" retrofitting solution among the 5 runs. These figures represent, on the left, the outcome of the proposed algorithm in terms of objective function vs counter of generation and, on the right, the time spent to achieve the stop condition. More specifically, the graphs on the left show the costs of the cheapest retrofit solution among the current population, until convergence. As shown, in both cases the objective function starts from a high cost and decreases progressively. As expected, the curve shows a very steep slope over the first 10 generations and a slower and slower reduction, characterized by a staircase shape, towards the stop condition. This condition is met at the 50$^{th}$ generation and 42$^{nd}$ generation, respectively in case of Lioni and L'Aquila.

For the case of the structure located in Lioni, the fittest chromosome in the 50$^{th}$ population has a total cost of 34,637 € which is the sum of the cost for "global" intervention $\boldsymbol{C_{glob}}$ (20,048 €) and the cost for the enlargement of the existing foundation system $\boldsymbol{C_{found}}$ (14,589 €).

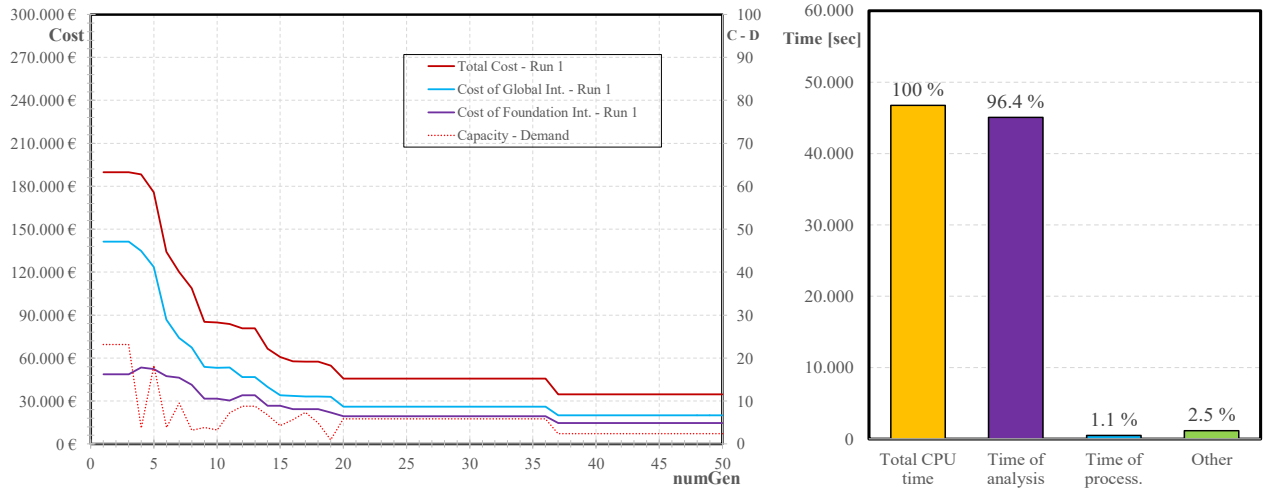


***Fig. 21**: Convergence history (left); and time profiling of the algorithm (right) for the case of Lioni*

Conversely, for the case of the structure in L'Aquila, the fittest chromosome in the 42$^{nd}$ generation has a total cost of 47,874 € which is the sum of the cost for "global" interventions $\boldsymbol{C_{glob}}$ (27,206 €) and the cost for the intervention on the existing foundation system $\boldsymbol{C_{found}}$ (20,668 €). As can be seen, the minimum among the 8 value of the $g_{LS}$ function (represented with the red dashed line) tends to approach the zero, meaning that the retrofitting solutions evolve towards full utilization of the supplied Capacity in both existing and newly designed members. As shown in the histogram on the right side, in both cases more than 96% of the computational time is spent by the OpenSEES program to perform the seismic analyses.

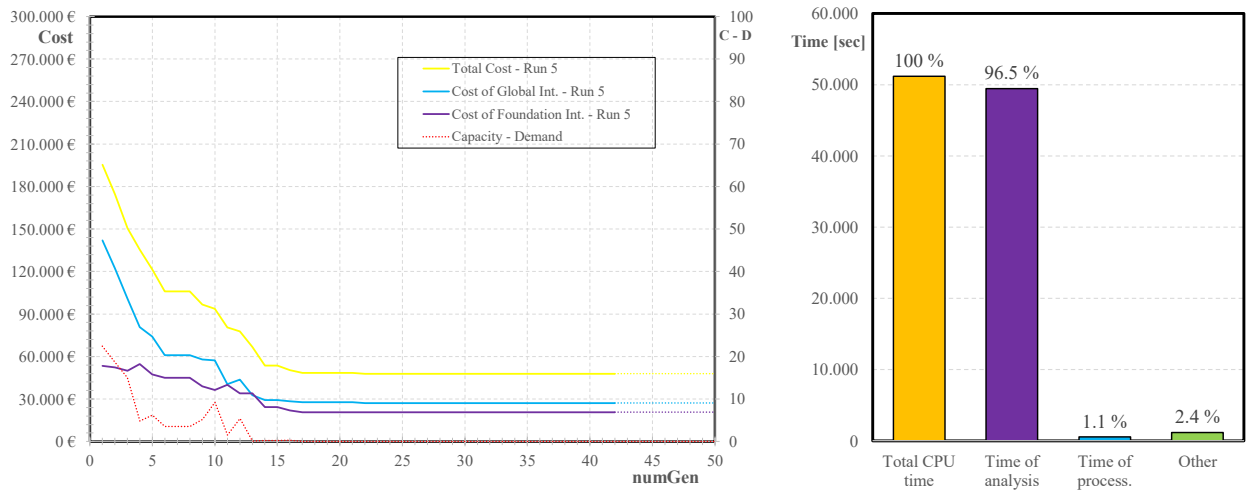


***Fig. 22**: Convergence history (left); and time profiling of the algorithm (right) for the case of L'Aquila*

Starting from the ***BestChrom*** belonging to the last generation, or in other words, the vector of the optimized decision variables $\boldsymbol{x}_{opt}$, it has been possible to "trace" the actual retrofit intervention by the defined mapping rule genotype → phenotype, as shown in Fig. 23 and Fig. 24.

In the case of Lioni, the best retrofit solution came up to consist of a purely global intervention (realized with two concentric steel bracing systems in the plain frame along the Y-direction and one bracing system in the X-direction), while no local FRP wrapping interventions are required. Moreover, 2 micro-piles ($\boldsymbol{N}_{mp,col}$) are required under the columns #7, #8, #12, #13, #18 and #19. The table on the right collects the "smallest" sections $A_i$ of steel members needed for each floor.

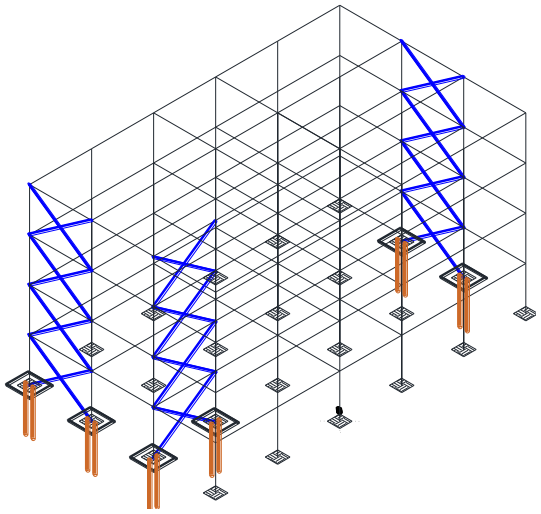

| | Floor | Area [cm$^2$] | Section |
|---|---|---|---|
| **Beam 10** | **1st** | 26.04 | HE 100 B |
| | **2nd** | 26.04 | HE 100 B |
| | **3rd** | 26.04 | HE 100 B |
| | **4th** | 26.04 | HE 100 B |
| **Beam 18** | **1st** | 34.01 | HE 120 B |
| | **2nd** | 26.04 | HE 100 B |
| | **3rd** | 26.04 | HE 100 B |
| | **4th** | 26.04 | HE 100 B |
| **Beam 24** | **1st** | 34.01 | HE 120 B |
| | **2nd** | 26.04 | HE 100 B |
| | **3rd** | 26.04 | HE 100 B |
| | **4th** | 26.04 | HE 100 B |

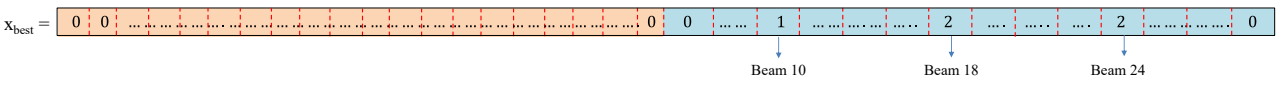


***Fig. 23**: Extrapolation of the BestChrom from the 45$^{th}$ generation and corresponding phenotype*

In the case of L'Aquila, again the "fittest" retrofit solution came up to consist of a purely global intervention (realized with two concentric steel bracing systems in the plain frame along the Y-direction and two bracing systems in the X-direction), while no local FRP interventions are required (Fig. 24). Moreover, 2 micro-piles are required under the columns #4, #5, #9, #10, #15, #16, #20, #21.

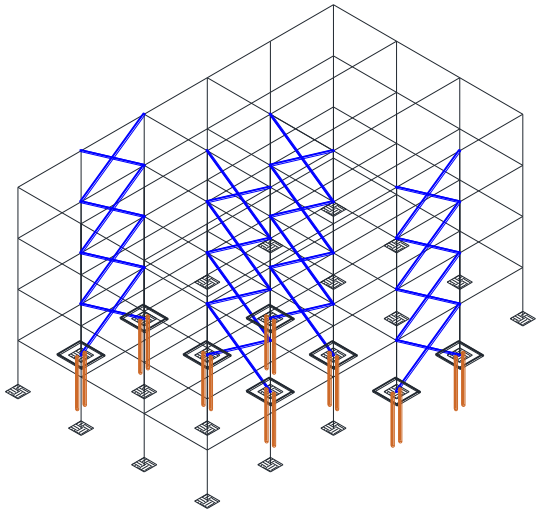

| | Floor | Area [cm$^2$] | Section |
|---|---|---|---|
| **Beam 4 Beam 17** | **1st** | 34.01 | HE 120 B |
| | **2nd** | 26.04 | HE 100 B |
| | **3rd** | 26.04 | HE 100 B |
| | **4th** | 26.04 | HE 100 B |
| **Beam 16** | **1st** | 42.96 | HE 140 B |
| | **2nd** | 26.04 | HE 100 B |
| | **3rd** | 26.04 | HE 100 B |
| | **4th** | 26.04 | HE 100 B |
| **Beam 29** | **1st** | 26.04 | HE 100 B |
| | **2nd** | 26.04 | HE 100 B |
| | **3rd** | 26.04 | HE 100 B |
| | **4th** | 26.04 | HE 100 B |

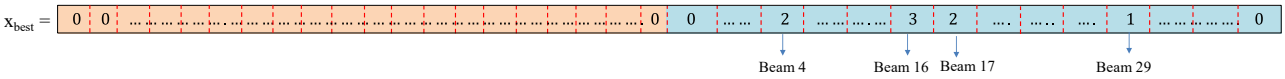


***Fig. 24**: Extrapolation of the BestChrom from the 42nd generation and corresponding phenotype*

For both case studies, the cheapest retrofit solution meets the performance constraints in Eq. (1) for each load patterns and for each Limit States considered, as shown in Fig. 25 and Fig. 26.

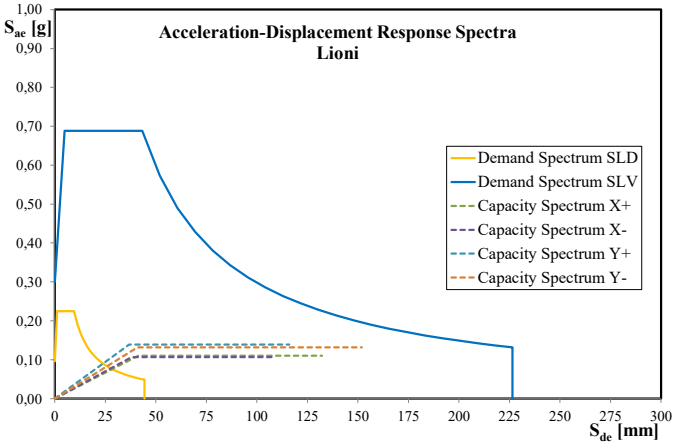


| | SLD $g_{LS}$ [mm] | SLV $g_{LS}$ [mm] |
|---|---|---|
| **Pushover X+** | 2.4 | 16.6 |
| **Pushover X-** | 2.9 | 3.4 |
| **Pushover Y+** | 9.9 | 6.2 |
| **Pushover Y-** | 2.7 | 42.9 |

***Fig. 25**: Values of Limit State function following the "cheapest" retrofit intervention (case of Lioni)*

This is mainly due to the enhancement of the original stiffness realized by the installation of bracing systems working in parallel with the existing structure.

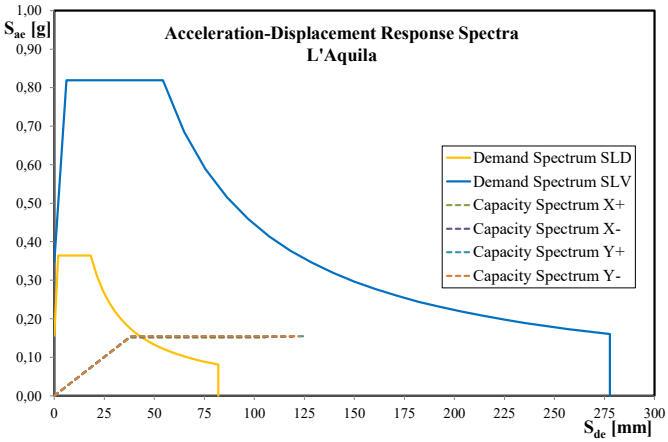


| | SLD $g_{LS}$ [mm] | SLV $g_{LS}$ [mm] |
|---|---|---|
| **Pushover X+** | 1.4 | 0.7 |
| **Pushover X-** | 0.7 | 18.9 |
| **Pushover Y+** | 0.1 | 27.2 |
| **Pushover Y-** | 0.9 | 23.8 |

***Fig. 26**: Values of Limit State function following the "cheapest" retrofit intervention (case of L'Aquila)*

## 4.2 Concluding remarks

This paper describes an automated GA-based procedure capable of selecting and designing the cheapest retrofit solution for existing vulnerable RC buildings. Although the proposed procedure could be extended to other retrofitting techniques, in this preliminary implementation the generic retrofit intervention is supposed to be realized through a possible combination of the confinement of columns (through FRP wraps) and the installation of concentric steel bracing systems. Since the total cost of intervention is assumed as the objective function, the procedure aims at returning the minimum number of FRP sheets needed to realize the local confinement, the "fittest" layout of bracing elements (both topology and size), and the minimum number of micro-piles required to realize the possible strengthening intervention on the foundation system. It is worth mentioning that the total CPU time obviously depends on the performance of the processor employed for the seismic simulations: obviously, the shorter elaboration time is required if more powerful computers are utilized to run the procedure. However, a restriction on the use of the procedure is currently necessary. In fact, in the case of T-shaped, L-shaped or C-shaped structures (where the center of gravity is located far from the center of rigidity) or structures enhanced through "asymmetric" interventions, pushover analysis (currently employed) cannot simulate the actual seismic response and, hence, the simulations of both the as-built configuration and the retrofitted structure can be somehow biased. As a future development, research efforts should focus on the search of the best suited seismic analysis as a trade-off between the accuracy of the response prediction (even for "irregular" case studies) and the computational time cost. Finally, as part of the future developments of the present research a more comprehensive objective function could be obtained by accounting not only the initial cost of intervention but a series of concurrent (for instance, including the

maintenance and life-cycle costs) or conflicting objectives based on both strictly quantitative measures or qualitative measures, possibly related to either the users' opinion or the aesthetical aspects of the final solution.

## Acknowledgments

The Authors wish to thank CE.MI. Srl, an Italian construction company, for co-funding the research assistant contract of the first author at the University of Salerno (contract call Prot. N. 186278 of 29/08/2018).

## Appendix

This appendix summarizes the general structure of the GA, whose pseudo-code is given below:

**Input**: Existing structure (FEM model), Seismic input (EDRS)

**Output**: Best chromosome

```
1  PopSize ← 100, numGen ← 1, maxGen ← 50, noImp ← 1, maxNoImpr ← 20
2  BestFit ← 0, BestChrom ← Ø, PopNew ← Ø, PopDisc ← 0.95*PopSize, μ_mut,1←0.05
3  Pop ← InitPop (PopSize),
4  while numGen ≤ maxGen OR noImp ≤ maxNoImpr do
5      for i ← 1 To PopSize do
6          RetrofitFE_i ← femodel (chromos_i)
7          OutPush_i ← seismic (RetrofitFE_i)
8          ObFunc_i ← postprocess (chromos_i, OutPush_i)
9          Fitness_i ← mapping (OutPush_i, ObFunc_i)
10     end
11     if maxfit (Pop) == BestFit then
12         noImp ← noImp +1
13     else
14         BestFit ← maxfit (Pop)
15         BestChrom ← findbest (Pop)
16         noImp ← 1
17     end
18     for i ← 1 To PopDisc/2 do
19         (P_1 , P_2) ← selection (Pop)
20         (O_1 , O_2) ← crossover (P_1 , P_2)
21         (O_M1 , O_M2) ← mutation (O_1 , O_2)
22         Insert ( [O_M1 , O_M2], PopNew)
23     end
24     Pop ← combine (Pop, PopNew)
25     numGen ← numGen + 1
26 end
27 return BestChrom
```

The procedure takes as input the FE model of the existing structure in its as-built configuration and an Elastic Demand Response Spectra representative of expected seismic demand. The main parameters of the algorithm are initialized at line 1 and 2. The first step (line 3) is the generation of an initial population Pop (whose counter

***numGen*** is set to 1) composed of a predefined number (***PopSize***) of individuals (candidate retrofitting interventions). Inside the ***while*** loop (line 4), for each individual (***chromos***$_i$) of the current population, the subroutine ***femodel*** (line 6) creates an updated FE model including the set of retrofitting interventions described by ***chromos***$_i$. Then, the subroutine ***seismic*** (line 7) simulates the response of the retrofitted structure subjected to the given seismic actions, the subroutine ***postprocess*** (line 8) evaluates the objective function and the constraints, and the subroutine ***mapping*** (line 9) evaluates the fitness function from the objective function of each individual. If the highest value of fitness among the current population ***BestFit***, obtained through the subroutine ***maxfit***, does not improve because it is the same of the previous population then the counter ***noImp*** is increased (line 12); otherwise, ***BestFit*** is updated and ***noImp*** is set again to one (line 16). The subroutine ***findbest***, instead, returns the best chromosome in the current population, i.e. the chromosome having the fitness equal to ***BestFit*** (line 15). The second "for" loop (line 18) aims at creating a new group of individuals for the following population. The loop includes the ***selection*** (line 19) of a pair of "parent" chromosomes ($P_1$ , $P_2$), ***crossover*** of their genetic information (line 20), and a possible ***mutation*** (line 21) leading to generate a pair of "offspring" chromosomes ($O_{M1}$ , $O_{M2}$). Each newly generated individual is inserted in the new population ***PopNew*** unconditionally, namely regardless of their fitness or belonging to ***Pop*** (line 22). According to the chosen reinsertion strategy, they take the place of the ***PopDisc*** discarded individuals (having the worst fitness function value). Once all the i-th matings have been realized, the subroutine ***combine*** assembles the survived individuals of ***Pop*** with the ones belonging to ***PopNew*** (line 24) into a new population ***Pop***. Thus, the counter of generation ***numGen*** is increased (line 25). The while loop iterates until either after ***maxNoImpr*** consecutive iterations without improvements of the ***BestFit*** value or after ***maxGen*** generations are reached (line 4). Once the stop condition is achieved, the fittest chromosome ***BestChrom*** in the last population is returned (line 26). Section 3 explains further details about the actual numerical implementations of the procedures.

# References


[1]. Kaplan, H., Bilgin, H., Yilmaz, S., Binici, H., Öztas, A. 2010. Structural damages of L'Aquila (Italy) earthquake. Natural Hazards and Earth System Sciences, 10(3), 499.

[2].European Standard EN (Eurocode 8) 1998-1:2005, Design of structures for earthquake resistance, Part 1: General rules, seismic actions and rules for buildings. European Committee for Standardization (CEN), Bruxelles, 2005.

[3].Elwood, K., Comartin, C., Holmes, W., Kelly, D., Lowes, L., Moehle, J. 2010. Program Plan for the Development of Collapse Assessment and Mitigation Strategies for Existing Reinforced Concrete Buildings (No. Grant/Contract Reports (NISTGCR)-10-917-7). National Institute of Standards and Technology, Gaithersburg.

[4].Bedon, C., Amadio, C. 2018. Numerical assessment of vibration control systems for multi-hazard design and mitigation of glass curtain walls. Journal of Building Engineering, 15, 1-13.

[5].fib .2003. Seismic assessment and retrofit of reinforced concrete buildings. Bulletin No. 24 138 ISBN: 978-2-88394-054-3.

[6].Rodriguez, M., Park, R. 1994. Seismic load tests on reinforced concrete columns strengthened by jacketing. Structural Journal, 91(2), 150-159.

[7].Priestley, M. J. N., Seible, F., Xiao, Y., and Verma, R. 1994. Steel jacket retrofitting of reinforced concrete bridge columns for enhanced shear strength. 1: Theoretical considerations and test design. ACI Struct. J., 91 (4), 394–405.

[8].fib. 2006. Retrofitting of concrete structures by externally bonded FRPs, with emphasis on seismic applications, Bulletin No. 35, 220, ISBN: 978-2-88394-075-8.

[9].Kaplan, H., Yilmaz, S., Cetinkaya, N., Atimtay, E. 2011. Seismic strengthening of RC structures with exterior shear walls, Sadhana, Indian Academy of Sciences , 36(1), 17–34.

[10].Sugano, S. 1982. An Overview of the State-of-the-Art in Seismic Strengthening of Existing Reinforced Concrete Buildings in Japan. In Proceedings of the Third Seminar on Repair and Retrofit of Structures, Ann Arbor, USA.

[11].Martinelli, E., Lima, C., Faella, C. 2015. Towards a rational strategy for seismic retrofitting of RC frames by combining member- and structure-level techniques. SMAR2015 – Third Conference on Smart Monitoring, Assessment and Rehabilitation of Civil Structures, Antalya (Turkey).

[12].Thermou, G.E., Elnashai, A.S. 2006. Seismic retrofit schemes for RC structures and local–global consequences, Progress in Structural Engineering and Materials, 8:1–15.

[13].Faella, C., Martinelli, E., Nigro, E. 2008. A rational strategy for seismic retrofitting of RC existing buildings, Proceedings of the fourteenth World Conference on Earthquake Engineering (14WCEE), October 12-17, Beijing, China.

[14].Chisari, C., Bedon, C. 2016. Multi-objective optimization of FRP jackets for improving the seismic response of reinforced concrete frames.Russell, S.J., Norvig, P., Canny, J.F., Malik, J.M., Edwards, D.D. 2003. Artificial intelligence. A modern approach. vol. 2. Prentice hall Upper Saddle River.

[15].Holland, J. H. 1975. Adaptation in natural and artificial systems. Ann Arbor, University of Michigan Press. Michigan.

[16].Darwin, C. 1859. The origin of species by means of natural selection. Murray. J. London.

[17].Mendel, G. 1866. Versuche über Pflanzenhybriden. Verhandlungen des naturforschenden Vereines in Brunn 4: 3, 44 (in German).

[18].Goldberg, D.E. 1989. Genetic algorithms in search, optimization and machine learning. Addison-Wesley Publishing Company Inc., New York, NY, USA, 432 pp.

[19].Coello, C. A., & Christiansen, A. D. 2000. Multiobjective optimization of trusses using genetic algorithms. Computers & Structures, 75(6), 647-660.

[20].Lagaros, N. D., Papadrakakis, M., Kokossalakis, G. 2002. Structural optimization using evolutionary algorithms. Computers & Structures. 80(7), 571-589.
[21].Falcone, R., Lima, C., Martinelli, E. 2018. Soft Computing techniques in structural and earthquake engineering: a literature review (submitted for publication in Engineering Structures).
[22].Bedon, C., Amadio, C. 2018. Numerical assessment of vibration control systems for multi-hazard design and mitigation of glass curtain walls. Journal of Building Engineering, 15, 1-13.
[23].McKenna, F., Fenves, G. L., Scott, M. H. 2000. Open system for earthquake engineering simulation. University of California, Berkeley, CA.
[24].Structural Engineers Association of California (SEAOC). 1995. Vision 2000, conceptual framework for performance-based seismic design. Recommended Lateral Force Requirements and Commentary, 1996, 6th Edition. Sacramento, CA: 391-416.
[25].M.II.TT. 2008 D.M. 14/01/2008 "Norme tecniche per le costruzioni", G.U. n. 29 04/02/2008 (in Italian).
[26].Cosenza, E., Manfredi, G., Verderame, G. M. 2002. Seismic assessment of gravity load designed rc frames: critical issues in structural modelling. Journal of Earthquake Engineering, 6 (spec01), 101-122.
[27].Roy, B., 1973. How outranking relation helps multiple criteria decision making, Multiple Criteria Decision Making, Actes du Séminaire «Théorie de la Décision», Beaulieu-Sainte-Assise, Francia.
[28].Caterino, N., Iervolino, I., Manfredi, G., Cosenza, E. 2008. Multi-criteria decision making for seismic retrofitting of RC structures. Journal of Earthquake Engineering, 12(4), 555-583.
[29].Kent, D. C., Park, R. 1971. Flexural members with confined concrete. Journal of the Structural Division, 97(7): 1969-1990.
[30].Taucer, F., Spacone, E., Filippou, F. C. 1991. A fiber beam-column element for seismic response analysis of reinforced concrete structures (Vol. 91, No. 17). Berkekey, California: Earthquake Engineering Research Center, College of Engineering, University of California.
[31].European Standard EN (Eurocode 3) 1993-1-1:2005, Design of steel structures, Part 1-1: General rules and rules for buildings. European Committee for Standardization (CEN), Bruxelles, 2005.
[32].Panagiotakos, T. B., Fardis, M. N. 2001. Deformations of reinforced concrete members at yielding and ultimate. Structural Journal, 98(2), 135-148.
[33].Fajfar, P., Fischinger, M. 1989. N2-A method for non-linear seismic analysis of regular buildings. In: Proceedings of the 9th world conference on Earthquake Engineering, Vol. 5. Tokyo- Kyoto: Japan; p. 111–116.
[34].Newmark, N. M., and Hall, W. J. 1982. Earthquake Spectra and Design. Engineering Monographs on Earthquake Criteria, Structural Design, and Strong Motion Records, Vol 3, Earthquake Engineering Research Institute, Oakland, CA.
[35].de Paula Garcia, R., de Lima, B. S. L. P., de Castro Lemonge, A. C., Jacob, B. P. 2017. A rank-based constraint handling technique for engineering design optimization problems solved by genetic algorithms. Computers & Structures, 187, 77-87.
[36].Bäck, T., Hoffmeister, F. Schwell, H.P. 1991. A Survey of evolution strategies, Proceedings of the Fourth International Conference on Genetic Algorithms, Morgan Kaufmann, 2-9.
[37].Jenkins, W.M. 1991. Towards Structural Optimisation via the Genetic Algorithm. Computers & Structures, 40(5): 1321–1327.
[38].De Jong, K. A. 1975. Analysis of the behavior of a class of genetic adaptive systems. (Doctoral dissertation, University of Michigan). Dissertation Abstracts International, 36(10), 5140B. (University Microfilms No. 76-9381).
[39].Syswerda, G. 1989. Uniform Crossover in Genetic Algorithm. Proceedings of 3th International Conference on Genetic Algorithm (ed. Schaffer, J.D.), Morgan Kaufmann, San Mateo, CA, 2-8.
[40].Yettram, A. L., Husain, H. M. 1965. Grid-Framework Method for Plates. Journal of the Engineering Mechanics Division, 91(3), 53-64.
[41].Berliner, H. J. 1981. An Examination of Brute Force Intelligence. In IJCAI, pp. 581-587.